Climate Dynamics (2026) 64:345
https://doi.org/10.1007/s00382-026-08305-x

ORIGINAL ARTICLE

Future elevation-dependent changes in meteorological variables across the european alps and their possible links to surface temperature: insights from the EURO-CORDEX ensemble

Anna Napoli[1,2] · **Michael Matiu**[1] · **Sven Kotlarski**[3] · **Dino Zardi**[1,2] · **Alberto Bellin**[1,2] · **Bruno Majone**[1]

Received: 28 October 2025 / Accepted: 3 July 2026 / Published online: 28 July 2026
© The Author(s) 2026

Abstract

Assessing future changes of weather-related variables in mountainous areas poses significant challenges, partly due to the inherent complexity of orographic effects and the associated atmospheric dynamics, which further amplify the difficulty. Additionally, mountains exhibit region-specific changes, making it essential to analyze single areas separately. In recent decades, elevation-dependent warming and its future projections have been studied extensively compared to other variables. However, understanding the drivers and interconnections among various elevation patterns requires a comprehensive analysis of results from model simulations. This study focuses on the European Alpine region and uses the large EURO-CORDEX ensemble to investigate elevation-dependent patterns of change between the historical period (1981–2010) and future projections (2071–2100, RCP8.5) across 18 climate variables, including surface and air temperature, long- and shortwave radiation, humidity, cloud cover, and snow cover. In particular, we assess whether these elevation-dependent patterns are consistent across simulations during the winter and spring seasons, and we investigate potential driving mechanisms behind these changes. We find strong elevation-dependent patterns for minimum temperature, diurnal temperature range, and specific humidity. Significant correlations are also observed between changes of surface temperature and diurnal temperature range, minimum temperature, specific humidity, downward longwave radiation, and shortwave radiation balance. These relationships exhibit a clear elevation dependence, possibly primarily driven by changes in snow cover and soil properties, which also influence surface heat fluxes. At the same time, the results indicate that variables heavily influenced by model parameterization (e.g. heat fluxes and snow cover fraction) exhibit little to no coherence within the ensemble. This underscores the importance of adopting an ensemble-based approach when developing climate scenarios for future adaptation plans in order to capture the full range of possible outcomes.

Keywords European alpine region · Elevation patterns · EURO-CORDEX · Future changes

1 Introduction

Mountain climates are strongly responding to global climate change, although often showing spatially non-uniform patterns (Pepin et al. 2015, 2022; Napoli et al. 2023b; Ferguglia et al. 2024). Indeed, these changes are known to affect mountain systems in different region-specific ways, posing significant challenges to our understanding of the underlying processes, and hence to our designing appropriate adaptation plans (Napoli et al. 2023b).

The European Alpine region is one of the most studied and analyzed mountain areas. This is due to the abundance of observation stations (Bongiovanni et al. 2024) and gridded observational datasets (e.g., Auer et al. 2007; Isotta

✉ Anna Napoli
anna.napoli@unitn.it

[1] Department of Civil, Environmental and Mechanical Engineering (DICAM), University of Trento, Via Mesiano, 77, Trento (TN) 38123, Italy

[2] Center Agriculture Food Environment (C3A), Via Edmund Mach, 1, San Michele all'Adige (TN) 38010, Italy

[3] Federal Office of Meteorology and Climatology, MeteoSwiss, Operation Center 1, Zurich-Airport CH-8058, Switzerland

et al. 2014; Crespi et al. 2021; Škrk et al. 2021; Hiebl and Frei 2018), as well as its high sensitivity and vulnerability to climate change. Between the late 19th century and the early 21st century, large portions of the Alpine range have experienced a warming rate higher than that observed in surrounding European land areas (Auer et al. 2007; Ceppi et al. 2012). However, the warming rate is not uniform in space: it varies with elevation, region, and even between the northern and southern sides of the Alps (Nigrelli and Chiarle 2023). Indeed, different parts of the Alps show contrasting patterns: in some areas, such as the eastern Italian Alps (Tudoroiu et al. 2016) and Switzerland during autumn and early winter (Scherrer et al. 2026), lower elevations have warmed more than higher elevations, primarily due to increased sunshine duration, and reductions in cloud, fog, and aerosol cover. Conversely, mid-elevations can exhibit slightly enhanced warming in spring, driven by snow-albedo feedbacks, as observed in Switzerland (Scherrer et al. 2026) and in the French Alps (Beaumet et al. 2021). At the same time, positive elevation-dependent warming has been documented at high altitudes in Valle d'Aosta (western Alps), based on permafrost changes (Pogliotti et al. 2023).

In time, not only the mean temperature has changed, but also the distribution of temperature minima and maxima, and consequently the Diurnal Temperature Range (DTR), an important indicator of climate change and a critical thermal metric to assess the impact climate warming on agriculture, human health (Cheng et al. 2014), vegetation (Gallou et al. 2023; Wang et al. 2023), and ecosystems (Barton and Schmitz 2018). Changes in the DTR over time show strong spatial and temporal variability, highlighting the local characteristics of different mountain regions (Mall et al. 2021; Zhao et al. 2024). In particular, in the European Alps (Weber et al. 1997) and parts of it (Piedmont region) (Rogora et al. 2004), climate warming mainly affected temperature minima, showing a non-univocal trend. In both studies, warming did not affect daily temperature extremes in the same way, resulting in a significant change over time in DTR values.

For precipitation, long-term changes and elevation dependencies vary across the Alpine region. The large decadal variability of precipitation in the Alps can modulate or even induce trends over long periods (Ménégoz et al. 2020), and such trends may differ spatially and seasonally (Blanchet et al. 2021; Kotlarski et al. 2022; Schmidli et al. 2002) exhibiting high spatial heterogeneity (Gobiet et al. 2014; Rysman et al. 2016). Moreover, extreme precipitation may respond differently from mean precipitation rates (Brönnimann et al. 2018), complicating the identification of the precipitation patterns and their associated changes in the region. Moreover, locally, precipitation changes vary across elevation ranges depending on the period and the considered regions (Napoli et al. 2019). Snow phenology has also been significantly influenced by global warming across different latitudes and elevations (Guo et al. 2026). Alpine snow cover and snow depth have declined substantially over recent decades due to climate-driven changes in temperature and precipitation, with reductions varying by season and elevation. These declines have become particularly pronounced at lower elevations in winter and at higher elevations in spring (Valt and Cianfarra 2010; Matiu et al. 2021).

Not only these variables changed in the past and continue to do so unevenly across elevations and valleys in the European Alps, but other key variables (such as radiation, heat fluxes, humidity, and cloud cover) play a fundamental role as feedbacks and drivers of many physical processes. In the Alpine range, surface solar radiation has increased over recent decades. This trend is attributed to a combination of reduced cloud cover and changes in atmospheric aerosols impacting different elevation bands (Manara et al. 2016; Schilliger et al. 2024). Humidity-related variables exhibit significant temporal and spatial variability: high-resolution measurements along an elevational gradient in the Italian Alps confirm the spatial variability of relative humidity within mountain environments (Zandonai et al. 2024), while recent continental-scale analyses indicate historical trends in both specific and relative humidity across Europe (Bilgili and Tokmakci 2025).

Understanding future changes in meteorological variables is crucial for assessing the impacts of climate change on environmental and socio-economic sectors at different elevation ranges (Napoli et al. 2026). Specifically, temperature and precipitation projections indicate that both summer and winter temperatures are expected to increase substantially across the European Alps by the end of the 21st century (Kotlarski et al. 2022), with increased warming at medium to high elevations, depending on the season (Kotlarski et al. 2022; Napoli et al. 2023a). In addition, a decrease of summer precipitation has to be expected, particularly in the southern Alpine range (Frei et al. 2018; Kotlarski et al. 2022; Coppola et al. 2021; Napoli et al. 2023a). Projected precipitation trends show a statistically significant relationship with elevation (Napoli et al. 2023a). Snow cover is also expected to decline markedly, with a marked elevation dependence, with strongest relative reductions in valley regions (Frei et al. 2018; Kotlarski et al. 2022). Winter precipitation is projected to slightly increase in the Alps and this might lead to core winter snowpack at high-elevation remaining constant; however, total seasonal snowpack is still found to decrease across all elevations (Kotlarski et al. 2022). In addition, future changes are expected in seasonal radiation and relative humidity (Gobiet et al. 2014), as well as in wind speed and direction, cloud cover, and the surface

energy budget (Pepin et al. 2022). However, the elevation dependency of these variables remains uncertain.

To better understand how climate change affects meteorological variables across elevation ranges in mountainous areas, it is essential to examine the physical drivers of these changes. Recent studies have explored the physical mechanisms driving temperature changes in various mountain regions worldwide, based on diverse datasets (e.g., Global Climate Models (Palazzi et al. 2017), observations (Williamson et al. 2020), and Regional Climate Models (Toledo et al. 2021)). In the European Alps, only a limited number of recent studies have investigated potential drivers of temperature (Tudoroiu et al. 2016; Ceppi et al. 2012) and precipitation changes (Kotlarski et al. 2022; Napoli et al. 2022, 2023a), emphasizing the need for more comprehensive analyses of the underlying processes influencing climate variability and climate change in these regions.

Surface temperature (ts) is a key variable that can be used to investigate the drivers of changes in temperature-related variables. As highlighted in several studies (e.g. Pepin et al. 2016), and assessment reports (e.g. IPCC and Chap 2021), surface temperature provides direct information on surface energy balance and land–atmosphere interactions, as the coupling between surface and near-surface air temperature is primarily governed by surface energy balance processes (CH2018 2018; Shati et al. 2018). Owing to its strong coupling with near-surface air temperature, it represents a valuable diagnostic variable for interpreting the dominant physical drivers of temperature.

In the present paper, we analyse the expected future changes in the European Alps using one of the most extensive climate modelling ensembles available over the region of interest, namely the European branch of the World Climate Research Programme's Coordinated Regional Climate Downscaling Experiment (EURO-CORDEX) ensemble (Jacob et al. 2014, 2020; Vautard et al. 2021). The analysis encompasses 18 climate variables and is thus the most comprehensive analysis available to date. Unlike existing studies on the European Alps (e.g., Kotlarski et al. 2022; Napoli et al. 2023a), we seek model (dis-)agreement on plausible physical mechanisms driving primarily surface temperature change. We focus our analysis on winter (DJF December-January-February) and spring (MAM March-April-May) seasons.

The paper is structured as follows. Section 2 describes the study area and the main climatic features. Section 3 presents the model data used in the study, along with the methods employed. Section 4 presents the results, followed by a discussion in Sect. 5. Finally, Sect. 6 presents the conclusions.

2 Study area

The study area refers to the region called the Greater Alpine Region (GAR), which includes the European Alps and their broader surroundings. This region is geographically defined approximately between $4-19°$E and $43-49°$N and comprises areas that are functionally and climatically connected to the Alpine system (Auer et al. 2007) (Fig. 1). The region analysed cover the Alpine range spans roughly 1200 km across central Europe, passing through countries such as France, Italy, Switzerland, Austria, Germany, and Slovenia. This region features a diverse and complex terrain, characterized by sharp peaks, deep valleys, and extensive plateaus. Iconic mountains, such as Mont Blanc (4809 m above sea level), the highest peak in Western Europe, and the Matterhorn (4478 m), highlight the dramatic relief of the Alps. These variations in elevation and the geographical location significantly influence the local climate, ecosystems, and hydrology of the area.

The climate of the Alpine range is shaped by a complex interplay of large scale and local factors. This extensive mountain system acts as a major natural barrier to atmospheric circulation, influencing both local dynamics—due to its complex topography—and large-scale weather patterns across Europe. The Alps are strongly affected by intense synoptic disturbances arriving from the Atlantic (Bertò et al. 2004; Bartolini et al. 2009; Zampieri et al. 2013), as well as by moist air masses originating from the Mediterranean Sea, a major moisture source for the surrounding land areas (Schicker et al. 2010). The northern Alps are predominantly influenced by Atlantic moisture, whereas the southern Alps receive a larger Mediterranean contribution (Sodemann and Zubler 2010; Giovannini et al. 2021), with these air masses forced to rise over the Alpine barrier. The resulting contrasts between the two sides of the mountain range make the Alpine region climatically very complex. Furthermore, climate patterns across both lowland and high-elevation areas

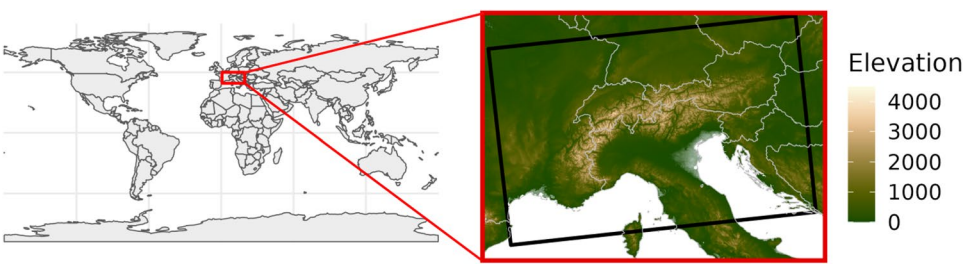


Fig. 1 Study area: the red box outlines part of Southern Europe, the European Alpine Region, while the black box highlights the primary focus area of the study. The elevation map of the area is shown in meters above sea level

Table 1 List of the variables analised in the study, which is composed by 14 variables downloaded from the EUROCORDEX raw ensemble and 4 computed. The acronym and the corresponding extended name are shown for each variable. Upward fluxes are considered positive

Extended name	Acronym
Minimum 2-meter air temperature	tasmin
Maximum 2-meter air temperature	tasmax
Surface temperature	ts
Precipitation	pr
Specific humidity	huss
Snow cover fraction	snc
Total cloud cover fraction	clt
Low level cloud cover fraction	cll
Surface Downwelling Shortwave Radiation	rsds
Surface Upwelling Shortwave Radiation	rsus
Surface Downwelling Longwave Radiation	rlds
Surface Upwelling Longwave Radiation	rlus
Surface Upward latent heat flux	hfls
Surface Upward sensible heat flux	hfss

are shaped not only by the region's geographical features but also by human activities, including aerosol loading (e.g. Napoli et al. 2022; Bigi et al. 2012; Guariso and Volta 2017) and land use/land cover (e.g. Barati et al. 2023; Ramtvedt et al. 2021).

3 Data and methods

3.1 Data

We analyzed 18 meteorological variables. Most of them (14) are downloaded from the public archive of the ensemble of GCM-driven EURO-CORDEX RCMs dataset (Jacob et al. 2014, 2020; Vautard et al. 2021), and the remaining (4) have been calculated to analyse the Diurnal Temperature Range and radiative budget, as described in Table 1.

The ensemble was downloaded from the Earth System Grid Federation (ESGF) servers between January 2023 and September 2024. Since in the present work we focus on elevation dependencies, we only employ the high-resolution EUR-11 sub-ensemble, characterized by a horizontal resolution of 0.11 degrees, corresponding to a grid cell width of approximately 12 km. In this study, we focused exclusively on the Representative Concentration Pathway 8.5 (RCP8.5). We evaluated multiple time periods and emission scenarios and identified the late-century period (2071–2100) under RCP8.5 as the most suitable, as it represents the strongest radiative forcing and thus allows elevation-dependent patterns to emerge more clearly as also reported by other recent studies as Kotlarski et al. (2022). Indeed, when considering temperature variables, differences between elevation bands become more pronounced, with the magnitude of projected changes showing a stronger and more consistent

Table 2 Overview table of the variables calculated and analysed from the EURO-CORDEX raw ensemble. The acronym, the extended name, and the definition are here reported. Upward fluxes are considered positive

Extended name	Acronym	Definition
Diurnal temperature range	DTR	tasmax-tasmin
Longwave radiative balance	LW_balance	rlds-rlus
Shortwave radiative balance	SW_balance	rsds-rsus
Net radiative balance	Net_balance	LW_balance+SW_balance

dependence on elevation. In addition, on the ESGF servers a larger ensemble of climate models is available for RCP8.5 compared to RCP4.5 and RCP2.6, further supporting this choice. The historical run of the RCMs, which ended in 2005, was merged with the RCP8.5 scenario, which started in 2006. We used the period 1981–2010 as a reference.

For the elevation analysis and the definition of land area, we used the surface elevation and the land area fraction outputs from each RCM. Only grid cells with a water fraction lower than 50% were considered, in order to include only land areas in the analysis.

All the simulations downloaded and analysed in the present work are reported in Table 3. Details on the model selection are provided in the Supplementary Material (Section S2).

3.2 Methods

The analysis is based on the comparison between the future (2071–2100) and the historical (1981–2010) climatological periods. Specifically, we analyzed the elevation-dependent change patterns of all the variables presented in Tables 1 and 2, after grouping them in the following 6 elevation classes: [0, 500), [500, 1000), [1000, 1500), [1500, 2000), [2000, 2500), $\geq$ 2500 m. The lower and upper bounds of each elevation class were determined through a sensitivity analysis, in which we evaluated both the number of bins and the number of pixels per bin (which could vary or be the same for each bin).

In this study, the change between the two periods was calculated either by subtracting the mean climatological value of the historical period from that of the future period, or by calculating the ratio of this difference to the historical period, expressed as a percentage (ratio).

Elevation class mean values were calculated for each model and each period, and the means of the models were computed for each variable as the average across all models. The elevation gradient was then estimated as a linear regression of the ensemble mean. The inter-model variability across GCM groups is reported in the Supplementary

Table 3 Combination of GCM and RCM used in this study for each variable from the EURO-CORDEX ensemble (Jacob et al. 2014, 2020; Vautard et al. 2021). The numbers at the bottom of the table represent the total number of simulations for the corresponding variable

institute	rcm_short	gcm_short	cll	clt	hfls	hfss	huss	pr	rlds	rlus	rsds	rsus	snc	tasmax	tasmin	ts
CNRM	ALADIN63	CNRM-CM5	v2	v2	v2	v2	v2	v2	v2	v2	v2	v2	v2	v2	v2	v2
CNRM	ALADIN63	HadGEM2-ES	v1	v1	v1	v1	v1	v1	v1	v1	v1	v1	v1	v1	v1	v1
CNRM	ALADIN63	MPI-ESM-LR	v1	v1	v1	v1	v1	v1	v1	v1	v1	v1	v1	v1	v1	v1
CNRM	ALADIN63	NorESM1-M	v1	v1	v1	v1	v1	v1	v1	v1	v1	v1	v1	v1	v1	v1
DMI	HIRHAM5	CNRM-CM5	v2	v2	v2	v2	v2	v2	v2	v2	v2	v2	v2	v2	v2	
DMI	HIRHAM5	EC-EARTH	v1	v1	v1	v1	v1	v1	v1	v1	v1	v1	v1	v1	v1	
DMI	HIRHAM5	HadGEM2-ES	v2	v2	v2	v2	v2	v2	v2	v2	v2	v2	v2	v2	v2	
DMI	HIRHAM5	IPSL-CM5A-MR	v1	v1	v1	v1	v1	v1	v1	v1	v1	v1	v1	v1	v1	
DMI	HIRHAM5	MPI-ESM-LR	v1	v1	v1	v1	v1	v1	v1	v1	v1	v1	v1	v1	v1	
DMI	HIRHAM5	NorESM1-M	v3	v3	v3	v3	v3	v3	v3	v3	v3	v3	v3	v3	v3	
GERICS	REMO2015	CNRM-CM5		v2	v2	v2	v2	v2	v2	v2	v2	v2		v2	v2	v2
GERICS	REMO2015	IPSL-CM5A-MR		v1	v1	v1	v1	v1	v1	v1	v1	v1		v1	v1	v1
GERICS	REMO2015	NorESM1-M		v1	v1	v1	v1	v1	v1	v1	v1	v1		v1	v1	v1
ICTP	RegCM4-6	CNRM-CM5	v2	v2	v2	v2	v2	v2	v2	v2	v2	v2		v2	v2	v2
ICTP	RegCM4–6	EC-EARTH	v1	v1	v1	v1	v1	v1	v1	v1	v1	v1		v1	v1	v1
ICTP	RegCM4–6	HadGEM2-ES	v1	v1	v1	v1	v1	v1	v1	v1	v1	v1		v1	v1	v1
ICTP	RegCM4–6	MPI-ESM-LR	v1	v1		v1	v1	v1	v1	v1	v1	v1		v1	v1	v1
ICTP	RegCM4–6	NorESM1-M	v1	v1	v1	v1	v1	v1	v1	v1	v1	v1		v1	v1	v1
MOHC	HadREM3-GA7–05	CNRM-CM5		v2	v2	v2	v2	v2	v2	v2	v2	v2		v2	v2	v2
MOHC	HadREM3-GA7–05	EC-EARTH		v1	v1	v1	v1	v1	v1	v1	v1	v1		v1	v1	v1
MOHC	HadREM3-GA7–05	HadGEM2-ES		v1	v1	v1	v1	v1	v1	v1	v1	v1		v1	v1	v1
MOHC	HadREM3-GA7–05	MPI-ESM-LR		v1	v1	v1	v1	v1	v1	v1	v1	v1		v1	v1	v1
MOHC	HadREM3-GA7–05	NorESM1-M		v1	v1	v1	v1	v1	v1	v1	v1	v1		v1	v1	v1
MPI-CSC	REMO2009	MPI-ESM-LR		v1	v1	v1	v1	v1	v1	v1	v1	v1		v1	v1	v1
SMHI	RCA4	CNRM-CM5	v1	v1	v1	v1	v1	v1	v1	v1	v1	v1	v1	v1	v1	v1
SMHI	RCA4	EC-EARTH	v1	v1	v1	v1	v1	v1	v1	v1	v1	v1	v1	v1	v1	v1
SMHI	RCA4	HadGEM2-ES	v1	v1	v1	v1	v1	v1	v1	v1	v1	v1	v1	v1	v1	v1
SMHI	RCA4	IPSL-CM5A-MR	v1	v1	v1	v1	v1	v1	v1	v1	v1	v1	v1	v1	v1	v1
SMHI	RCA4	MPI-ESM-LR	v1a	v1a	v1a	v1a	v1a	v1a	v1a	v1a	v1a	v1a	v1a	v1a	v1a	v1a
SMHI	RCA4	NorESM1-M	v1	v1	v1	v1	v1	v1	v1	v1	v1	v1	v1	v1	v1	v1
			21	30	29	30	30	30	30	30	30	30	16	30	30	24

Material (Section S3). Although the relationship between the target variables and elevation is not expected to be strictly linear, this approach provides an initial assessment of changes in elevation patterns between the two periods. This method is commonly used in studies investigating elevation-dependent variations in climate variables (e.g. Napoli et al. (2023a); Ferguglia et al. (2024); Palazzi et al. (2019)). The significance of the mean–elevation relationship was evaluated using a permutation test (1000 random shuffles) under the null hypothesis of no dependence. Results were considered statistically significant for p-values lower than 0.05 ($p < 0.05$).

To better understand possible links between environmental variables and their elevation patterns, scatterplots of projected changes in the variables have been analysed. The correlation between variables was calculated using the Pearson correlation coefficient.

4 Results

In this section, we present the main results for the winter (December–January–February, DJF) and spring (March–April–May, MAM) seasons. These periods are characterised by pronounced elevation-dependent temperature gradients compared to other seasons (Pepin et al. 2015, 2025) enabling a clearer identification of the dominant temperature drivers. Furthermore, these seasons are particularly relevant for mountain ecosystems and hydrology, as snow processes play a key role (Edwards et al. 2007; Fayad et al. 2017). As a result, focusing on DJF and MAM provides a comprehensive representation of the underlying dynamics.

4.1 Overall temperature changes and their elevation dependencies

Figure 2a shows the difference between the seasonal mean of the daily maximum (first row), minimum (second row) and surface (third row) air temperature between the future and the historical period. The seasonal means are averaged over the entire reference period and across all models. The changes of the long-term seasonal means of the minimum (tasmin) and surface (ts) daily temperatures show a similar spatial pattern: in winter (DJF), more pronounced changes are observed at mid-elevations (from 1000 to 1500 m), particularly on the southern side of the Alpine range. In contrast, in spring (MAM), the magnitude of these changes is generally smaller, though differences between the two sides of the Alpine range persist. Additionally, in both seasons, the south-western sub-range of the Alps exhibits stronger changes (darker colors) compared to other regions of the European Alps. The difference between the long-term average of the daily maximum air temperature in the two periods shows a different pattern: the magnitude of changes is smaller compared to tasmin and ts across the Alps. However, in winter, the changes are always more pronounced to the Italian and French sides of the Alps between 500 and 1500 m. In spring, the largest changes are observed between 1000 and 2000 m across the entire Alpine region. These differences in changes between tasmin and tasmax influence the pattern of changes in the Diurnal Temperature Range (DTR), as shown in Fig. 2b. We notice positive changes (i.e., larger DTR values in the future period), as evidenced by warm colors, in the regions north and south of the Alpine chain and contrasting negative changes across the Alps. However, while in winter (DJF) the signal is strong above 1000 m, as evidenced by the widespread dark blue color, in spring (MAM) the negative differences are evident at elevations above 1500 m across the Alps. This suggests a larger increase in the minimum daily temperature than the maximum daily temperature, as discussed below.

As shown in Table 4, presenting the mean change between future and historical periods of DTR, tasmin, tasmax, and ts, in DJF the future projection exhibits a greater increase in minimum daily temperature (+5.36±0.86°C) than in maximum daily temperature (+4.33±0.68°C), thereby leading to a decrease in the Diurnal Temperature Range (−1.02±0.55°C). Indeed, a decrease in DTR indicates that the temperature range between day and night is projected to be narrow across the Alpine region. This effect is more pronounced in winter than in spring. This pattern depends on elevation (Table 4): highlands higher than 1000 m are expected to experience more pronounced increases in temperature minima than lowland areas, less than 500 m. Consequently, while low elevations exhibit a positive change in DTR (+0.19±0.31°C in DJF and +0.18±0.33°C in MAM), the more substantial warming at high elevations yields a negative average DTR change across the entire Alpine region (−1.58±0.69°C in DJF and −0.65±0.34°C in MAM).

The daily mean surface temperature shows an intermediate pattern between tasmin and tasmax, as it reflects an average of day- and nighttime conditions and represents ground temperature, whereas tasmin and tasmax capture the daily extremes (see Table 4).

To better understand the differences across elevation ranges, Fig. 3 presents the mean changes as a function of elevation class. The greater variability found at higher elevations is likely due to the smaller sample size compared to lower elevations, resulting from the smaller number of grid cells in the respective elevation bands. Nonetheless, a strong consistency is evident across the RCM models. DTR and tasmin show significant elevation-dependent changes in both seasons. On average, DTR decreases by $-0.90\,^{\circ}C\,km^{-1}$ in DJF and $-0.80\,^{\circ}C\,km^{-1}$ in MAM,

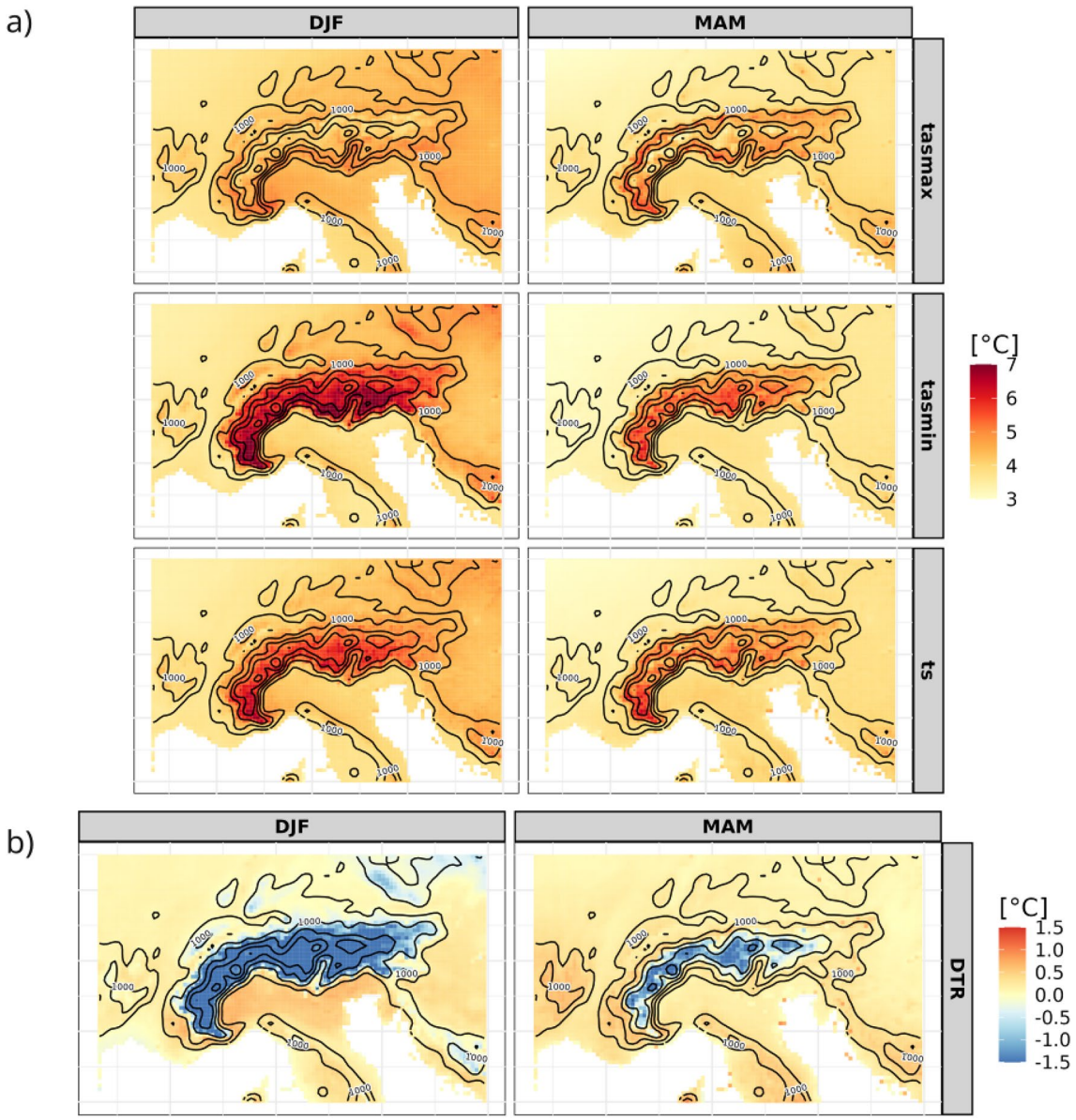


Fig. 2 Maps of the mean change in DJF and MAM between future (2071–2100, RCP8.5) and historical (1981–2010) periods of daily temperatures (tasmin, tasmax, ts) (**a**), and Diurnal temperature Range (**b**). The isolines are drawn every 500 m starting from 500 m

while tasmin increases by $+0.91\,°C\,km^{-1}$ in DJF and $+0.84\,°C\,km^{-1}$ in MAM. Surface temperature changes show a significant positive trend with elevation in DJF ($+0.68\,°C\,km^{-1}$), but no significant trend in MAM. In contrast, tasmax does not show any statistically significant pattern with elevation in either season. Notably, all the analyzed temperature variables exhibit elevation patterns with more pronounced increases or decreases at mid-elevations, which vary depending on the season and the specific variable considered. Maximum changes in the ensemble mean in DJF are found between 1500–2000 m a.s.l. for tasmin ($+6.4\,°C$) and DTR ($-2.0\,°C$), between 2000-2500 m a.s.l. for ts ($+5.6\,°C$), and between 1000-1500 m a.s.l. for tasmax ($+4.6\,°C$). ($+5.4\,°C$), between 1500-2000 m a.s.l. for ts ($+5.1\,°C$) and tasmax ($+4.9\,°C$), while DTR shows a reversal of the altitude-dependent trend in the mid-elevation range (about 1500 m a.s.l.).

4.2 Elevation dependencies of possible drivers of surface and air temperature change

As strong consistency has been found for the air and surface temperature changes and their elevation dependency in all simulations of the EURO-CORDEX ensemble, we investigate here whether the same consistency is observed for

Table 4 Mean change between future (2071-2100, RCP8.5) and historical (1981–2010) periods of Diurnal Temperature Range (DTR), minimum temperature (tasmin), maximum temperature (tasmax) and surface temperature (ts) with the corresponding model variability (one standard deviation). The values shown are calculated over the entire domain, and further distinguished between lowlands (from 0 to 500 m) and high elevation (higher than 1000 m)

	DTR [°C]	tasmin [°C]	tasmax [°C]	ts [°C]	
DJF	−1.02±0.55	+5.36±0.86	+4.33±0.68	+4.94±0.65	Entire
MAM	−0.35±0.27	+4.47±0.64	+4.12±0.56	+4.37±0.58	alpine region
DJF	+0.19±0.31	+3.96±0.53	+4.15±0.39	+3.98±0.40	Low-
MAM	+0.18±0.33	+3.48±0.40	+3.66±0.56	+3.62±0.49	lands
DJF	−1.58±0.69	+5.96±1.07	+4.37±0.84	+5.35±0.78	High
MAM	−0.65±0.34	+4.95±0.80	+4.30±0.63	+4.71±0.86	elevations

variables that could impact or cause air and surface temperature changes.

4.2.1 Clouds, humidity, precipitation, and snow cover

The relative changes in cloud cover (total and low-level cloud cover), specific humidity, total precipitation, and snow cover fraction as a function of the elevation are shown in Fig. 4. As expected, a decrease is projected in all elevation ranges for the snow cover fraction in both seasons, with higher relative values at lower elevations, characterised by a climatological smaller amount of snow compared to higher elevations. As shown in Fig. 4, total winter precipitation change (pr) decreases with the elevation ($-2.41\%\, km^{-1}$) but with an overall increase of +14.46%. On the other hand, total spring precipitation change shows a small overall increase (+2.48%) with a maximum increase of about $+3.15\%\, km^{-1}$ at mid-high elevation classes (1000–2500 m). Cloud cover change shows no statistically significant change with the elevation in DJF where the mean change over the entire region is +1.08% for clt and −0.72% for cll (see Table 1 for the meaning of the acronyms). In spring, changes in both cloud variables are decreasing when averaged across the entire study area (clt −3.43%, cll −8.19%), showing a statistically significant trend with the elevation for low-level cloud cover ($+1.76\%\, km^{-1}$). Specific humidity is projected to increase in the future in both seasons (DJF +38.67%, MAM +28.95%): all the simulations are coherent with the elevation pattern showing stronger changes at higher elevations in both seasons (maximum value +44.1% between 2000–2500 m a.s.l. in DJF, and +33.5% between 1500–2000 m a.s.l. in MAM), with significant elevation trends (DJF $+5.90\%\, km^{-1}$ MAM $+5.00\%\, km^{-1}$), a pattern that is consistent with the temperature profiles.

4.2.2 Radiation components

Fig. 5 shows the changes in the upward and downward radiation components. For long-wave radiation (rlds, rlus), a net positive change is observed across the entire region both in winter (+9.65%, +8.00% respectively) and in spring (+7.66% and +6.74% respectively), with significant

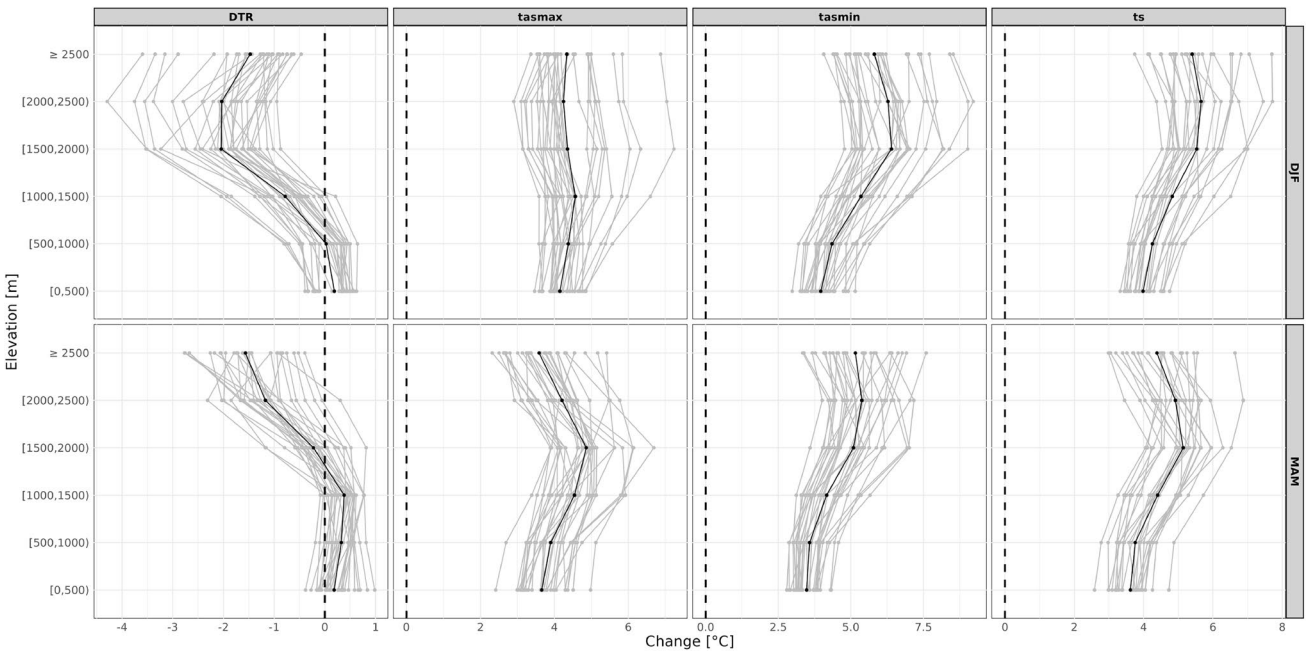


Fig. 3 Winter and Spring elevation pattern of the mean change between future (2071–2100) and historical (1981–2010) periods of Temperatures (tasmin, tasmax, ts) and DTR. The grey lines represent all the individual simulations, while the black line is the ensemble mean. A significant test has been applied to the mean changes with the elevation, as presented in Sect. 3.2

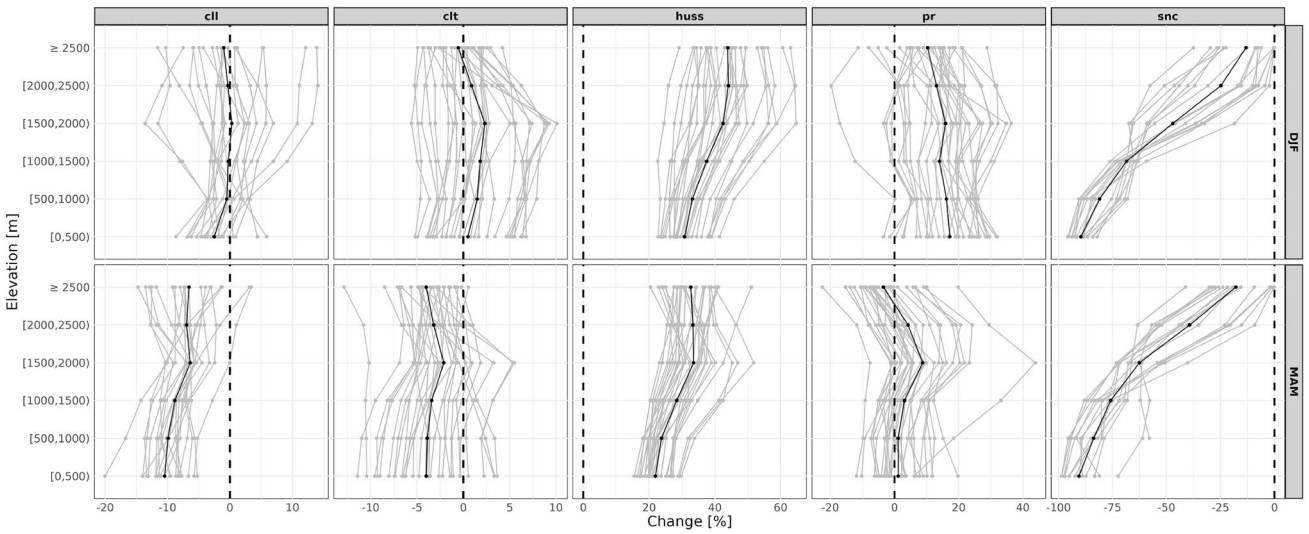


Fig. 4 Winter and Spring elevation pattern of the climatological mean change in percentage between future and historical periods of cloud cover (low-level and total, respectively cll and clt), specific humidity (huss), precipitation (pr) and snow cover fraction (snc). The grey lines represent all the simulations, while the black line is the mean over the entire simulation ensemble. A significant test has been applied to the mean changes with the elevation, as presented in Sect. 3.2

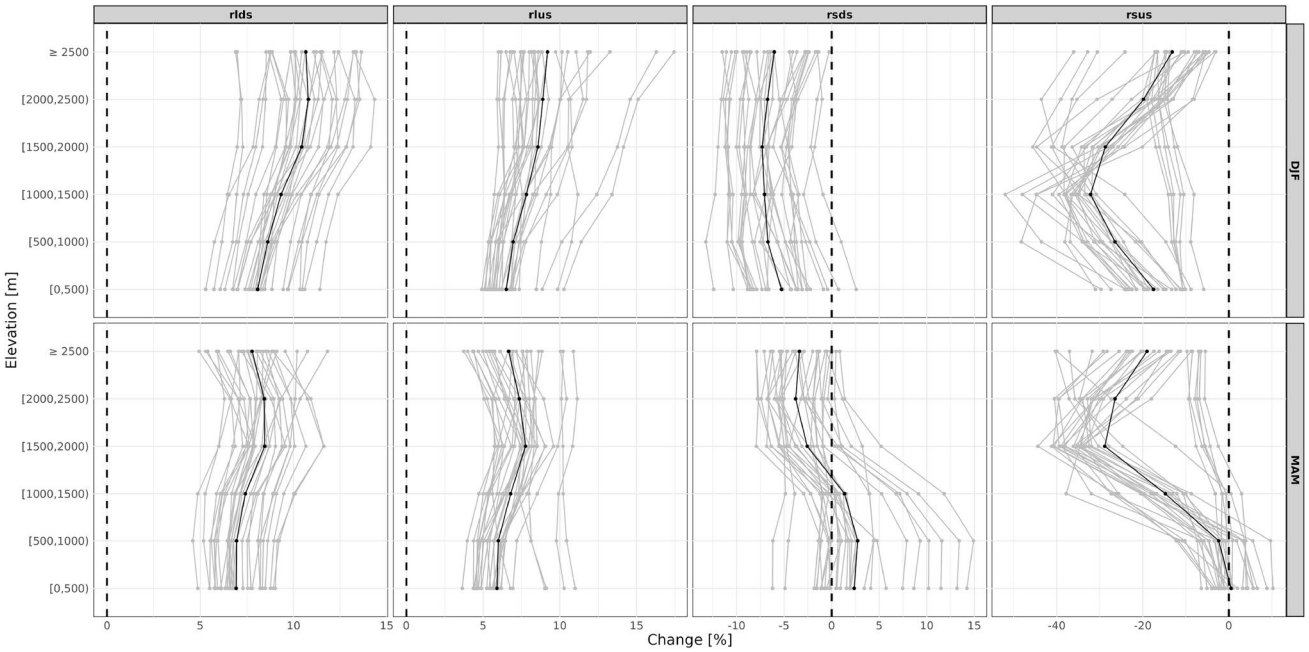


Fig. 5 Winter and Spring elevation pattern of the climatological mean change in percentage between future and historical periods of radiative components: long-wave downward (rlds), long-wave upward (rlus), short-wave downward (rsds), short-wave upward (rsus). The grey lines represent all the simulations, while the black line is the mean over the entire simulation ensemble. A significant test has been applied to the mean changes with the elevation, as presented in Sect. 3.2. Upward fluxes are considered positive

dependence on elevation in winter ($+1.17\%\,km^{-1}$ for rlds, and $+1.14\%\,km^{-1}$ for rlus). In MAM the maximum changes are between 1500-2000 m a.s.l. for rlds (+8.5%), and rlus (+7.8%). In contrast, short-wave radiation components (rsus and rsds) show higher model variability and stronger elevation patterns. In winter, mean changes in both downward and upward short-wave radiation are predominantly negative (−6.52% for rsds and −23.00% for rsus). The downward component displays high model variability but a coherent pattern with elevation, whereas the upward component varies more significantly based on model parameterizations and shows different elevation patterns. For rsus, most simulations indicate a stronger decrease from low to mid-elevations, followed by an

increase at higher elevations, though a few models suggest a slight linear decline with elevation. In spring, downward and upward short-wave radiation is characterised by a significant trend with the elevation: $-3.00\%\,km^{-1}$ for rsds and $-15.14\%\,km^{-1}$ for rsus.

4.2.3 Radiative balance and heat fluxes

Temperature variations are more accurately assessed by analyzing the absolute changes in heat fluxes and radiation budgets rather than their percentage changes. This approach is justified by the fact that heat fluxes and radiation budgets are expressed in specific units (W m^{-2}), and their absolute changes more directly correspond to (absolute) temperature shifts. For this reason, Fig. 6 shows the absolute changes.

Positive values indicate upward surface heat fluxes, while negative values signify fluxes directed toward the terrain (downward). The modelled climatology for these fluxes in the historical reference period is shown in the Supplementary Material (Section S1), where it is notable that the latent heat fluxes are positive during both winter and spring seasons, with a strong elevation dependency primarily in the MAM season. Conversely, sensible heat fluxes are generally negative across all elevations during winter months but become positive in spring. As illustrated in Fig. 6, which reports the changes of heat fluxes and radiative balance between future and historical simulations, the latent heat flux (hfls) increases across all elevation bands (mean average of $+2.79\,\mathrm{W\,m^{-2}\,km^{-1}}$ in DJF and $+8.50\,\mathrm{W\,m^{-2}\,km^{-1}}$ in MAM). While the simulations show consistent patterns for DJF, with slightly positive changes at low elevations and small to no changes at mid-to-high elevations, the results for MAM display greater variability among simulations. However, all simulations consistently indicate an increase at mid-elevations, followed by a decrease at higher elevations, resulting in an overall non-significant linear trend with elevation. For sensible heat fluxes, no substantial change is projected for winter ($+0.74\,\mathrm{W\,m^{-2}\,km^{-1}}$), which suggests that similar downward fluxes will also persist in the future during winter. However, in MAM, higher elevations are expected to experience increased sensible heat fluxes compared to historical values, though the trend with elevation is statistically not significant.

Figure 6 also illustrates changes in the radiative balance (long-wave, short-wave, and net), with climatological values available in the Supplementary Material (Section S1): it is important to note that, on average, the historical climatology of the long-wave budget is predominantly negative in both seasons, while the short-wave budget is positive, exhibiting notable differences in magnitude between DJF and MAM. As a result, the net radiative budget is close to zero in winter and positive in spring. This context is essential for interpreting the projected changes in these radiative balances shown in Fig. 6. The future change in the long-wave budget shows no statistically significant elevation-dependent patterns, with an average increase of $+1.85\,\mathrm{W\,m^{-2}\,km^{-1}}$ (about +4.6% relative to the historical climatology of the LW_balance) in DJF and approximately no change with the historical mean value in MAM. In contrast, the short-wave radiative balance displays more pronounced patterns with elevation, especially in MAM, where high-elevation areas are projected to experience increases

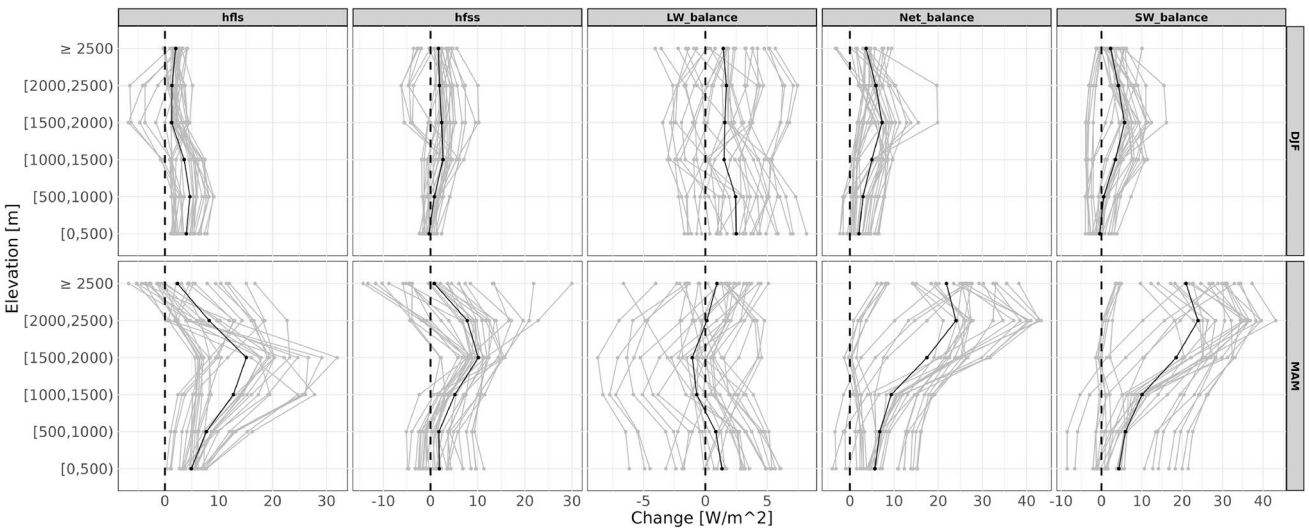


Fig. 6 Winter and Spring elevation pattern of the climatological mean change between future and historical periods of heat fluxes (latent heat and sensible heat, respectively hfls and hfss) and radiative balance (long-wave, short-wave and net, respectively LW_balance, SW_balance, Net_balance). Positive LW_balance and SW_balance mean that the surface is warmed by the atmosphere. The grey lines represent all the simulations, while the black line is the mean over the entire simulation ensemble. A significant test has been applied to the mean changes with the elevation, as presented in Sect. 3.2

of the budget exceeding $20\,\mathrm{W\,m^{-2}}$ which is roughly 30% increase over the historical mean at these elevations. The trend with the elevation of the mean for the SW_balance is statistically significant in MAM ($+8.31\,\mathrm{W\,m^{-2}\,km^{-1}}$): notice that only three models are not coherent with all the others in representing the elevation pattern of the budget. The pattern of the net balance largely mirrors that of the short-wave. These results suggest that in the future long-wave radiation components will change, but basically with no significant change in the balance between downward and upward radiation, while for short-wave radiation the future decrease of the components (see Fig. 5) will lead to stronger positive changes in the balance at higher elevations. This interesting behavior is better discussed in the Discussion section.

5 Discussion

5.1 Links between air temperature variables and surface temperature

The minimum temperature represents nighttime conditions, during which the Planetary Boundary Layer (PBL) is usually stably stratified and weakly mixed, so air temperatures at lower levels closely follow the surface temperature. In contrast, the maximum temperature occurs during daytime, usually in the afternoon, when the PBL is more turbulent, linking tasmax to surface temperature under more mixed conditions. This is shown in our study by the high correlation between changes in tasmin and ts both in winter ($r = 0.92$, $p< 0.05$; Fig. 7b) and spring ($r = 0.80$, $p< 0.05$; Fig. 8b), while the correlation between ts and tasmax is higher in spring ($r = 0.85$, $p< 0.05$; Fig. 8c) than in winter ($r = 0.68$, $p< 0.05$; Fig. 7c), likely reflecting the stronger daytime PBL mixing in spring that enhances the coupling between ts and tasmax.

The diurnal temperature range (DTR) reflects the combined behaviour of daily minimum and maximum temperatures. The strong negative correlation between changes in minimum temperature and DTR (DJF: $r = -0.83$, $p< 0.05$; MAM: $r = -0.67$, $p< 0.05$) indicates that the larger changes in tasmin compared to tasmax could play a dominant role in driving the reduction of DTR during these seasons. Indeed, changes in tasmax show little correlation with DTR (DJF: $r = 0.01$; MAM: $r = 0.19$). Similar behaviour between tasmin and tasmax changes has been reported in other regions, such as India (Mall et al. 2021) and China (Zhao et al. 2024), where global warming has been found to affect more strongly temperature minima than maximum. This asymmetric warming leads to a reduction in the diurnal temperature range, resulting in a negative trend of DTR. The seasonal variation in the correlation between DTR and surface temperature can be explained by the changing relative contributions of tasmin and tasmax, which are differently correlated with ts in different seasons as explained above. In winter, ts is more strongly linked to tasmin, resulting in a high correlation between DTR and ts ($r = -0.73$, $p< 0.05$, Fig. 7a). In spring, tasmax contributes more to DTR, so that the correlation between DTR and ts decreases ($r = -0.28$, $p< 0.05$, Fig. 8a), as DTR is now controlled by both tasmin and tasmax rather than primarily by tasmin.

All temperature variables exhibit major changes at mid-elevations, as shown in Figs. 7a, b, c and 8a, b, c and discussed in Sect. 4. This behaviour is consistent with the framework of elevation-dependent warming, as reported in previous studies such as Pepin et al. (2015) and, for the Alpine region, Kotlarski et al. (2022) and Kuhn and Olefs (2020). Rather than showing a fixed elevation of maximum change, the vertical structure of temperature trends appears to vary depending on the season and the analysed period. In our case, distinct patterns emerge between winter and spring, particularly for tasmax, which in turn influences the peak in DTR changes. This suggests that different physical mechanisms dominate in different seasons, leading to variations in the elevation at which maximum changes occur (Pepin et al. 2025). Observational studies in Switzerland (Rottler et al. 2021) support this interpretation, showing that temperature trends depend on season, elevation, and time of day, with the strongest warming occurring in spring and being particularly pronounced for daytime maximum temperatures. This seasonal signal has been linked to changes in downward solar radiation, cloud cover, and the frequency of specific weather types (Scherrer et al. 2026).

5.2 Links between specific humitidy, long-wave downward radiation and surface temperature

In our study, changes in ts are closely correlated with changes in specific humidity (huss) and in long-wave downward radiation (rlds), particularly in winter (Fig. 7f and i), respectively $r = 0.91$ ($p< 0.05$) and $r = 0.84$ ($p< 0.05$). These correlations also strongly depend on elevation, with larger surface temperature changes found at higher elevations compared to lowlands, where both huss and rlds show also more pronounced future changes, compared to the historical climatology. A similar but slightly weaker correlation is found in MAM (Fig. 8f and i), with values of 0.79 ($p< 0.05$) and 0.69 ($p< 0.05$) for huss and rlds, respectively. As also found in the Tibetan Plateau by Rangwala (2013), this pattern may be attributed to future changes in atmospheric humidity due to climate change. At high elevations, absolute changes in huss are smaller than at low elevations. However, the relative percentage change is larger (see Fig. 4), likely

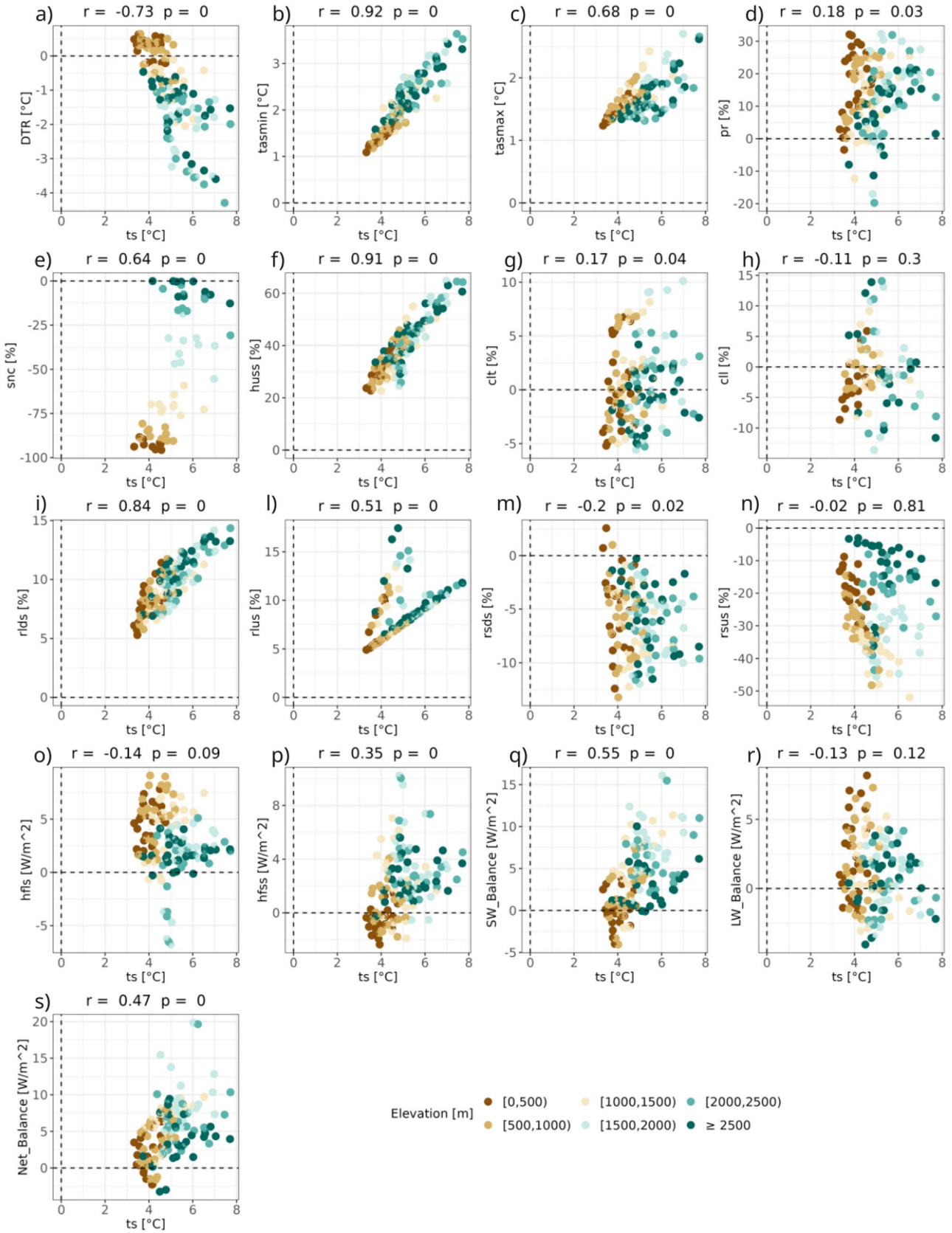


Fig. 7 Changes in DJF: scatterplot between all the variables analysed for each elevation class of each simulation and surface temperature. The relative correlation is in the panels (r). Different colors represent the different ranges of elevation

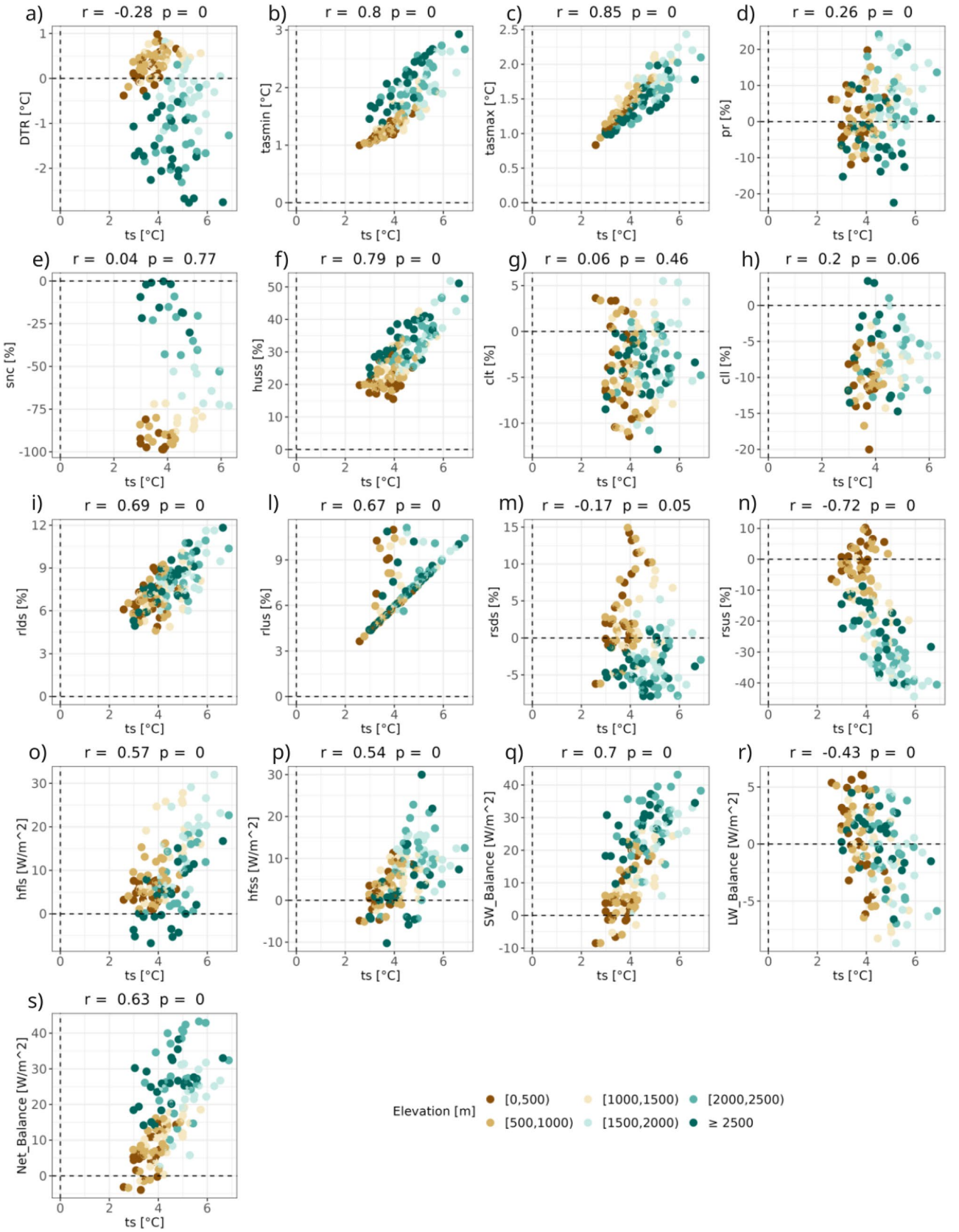


Fig. 8 Changes in MAM: scatterplot between all the variables analysed for each elevation class of each simulation and surface temperature. The relative correlation is in the panels (r). Different colors represent the different ranges of elevation

because high-elevation areas are characterized by colder and drier air masses and therefore lower baseline humidity. This substantial percentage change at high elevations significantly influences the long-wave downward radiation, a parameter highly sensitive to humidity levels (Zhang et al. 2024), in a non-linear and non-proportional manner (Palazzi et al. 2019), and that has emerged as the most remarkable contributing factor in controlling surface temperature change in mid-high latitudes of the Northern Hemisphere (Zhang et al. 2024). Consequently, these two factors impact surface temperature by increasing the long-wave radiation received from the atmosphere, affecting ts, tasmin, and the diurnal temperature range. As also reported in the EDCC review (Pepin et al. 2025), changes in specific humidity and downward longwave radiation in model simulations are more relevant for EDW in winter than in spring, likely due to drier atmospheric conditions. In our study, the signal is consistent across all simulations and shows a maximum change at approximately 2000 m a.s.l. (see Figs. 3, 4, and 5). However, the resulting pattern of humidity change does not exhibit a monotonic dependence on elevation, as it tends to level off above mid-elevations, forming a plateau rather than a continued increase. This behaviour suggests that the signal cannot be explained solely by a proportional response to changes in humidity with elevation. While humidity-driven effects would be expected to produce a more monotonic scaling, the observed plateau indicates that additional physical constraints and processes become increasingly relevant above mid-elevations.

5.3 Links between upward long-wave radiation, short-wave components and surface temperature

The other unidirectional long-wave radiation component (upward) is weakly correlated with ts in DJF ($r = 0.51, p < 0.05$, Fig. 7l), while no correlation is present for short-wave components (rsds: $r = -0.2$, $p < 0.05$; rsus: $r = 0.02$, $p < 0.05$; Fig. 7m, n) which also do not show a coherent signal across all simulations as a function of elevation. In spring season, except for rsds, radiation components are characterised by higher correlation coefficients (rlus: $r = 0.67$, $p < 0.05$; rsus: $r = -0.72, p < 0.05$; Fig. 8), likely because these components may not directly drive changes in surface temperature, but rather tend to respond to its variations.

5.4 Links between precipitation, cloud cover and surface temperature

Despite potential physical feedbacks among variables, seasonal changes in cloud cover and precipitation exhibit weak correlations with surface temperature changes and do not show a coherent elevation-dependent structure across simulations (Figs. 7d, g, h, and Fig. 8d, g, h). This suggests that their relationship with surface temperature is not primarily governed by a simple co-variation with elevation, but rather reflects more complex and potentially decoupled processes within the EURO-CORDEX ensemble. Alternatively, it may indicate that changes in water vapor play a more important role in driving surface temperature changes than cloud cover (Zhang et al. 2024).

5.5 Links between snow cover and surface temperature

An interesting pattern is observed for snow cover, a key variable in mountain environments. As shown in several studies over the European Alps (e.g. Beaumet et al. 2021; Marty 2013; Marty et al. 2017), low elevations experience, and are projected to experience, larger relative changes in snow cover compared to high elevations, mainly due to differences in baseline climatological snow conditions (Fig. 4). In winter, the percentage change in snow cover fraction is significantly correlated with surface temperature changes ($r = 0.64, p < 0.05$; Fig. 7e) and also exhibits a clear elevation dependence, with larger temperature increases associated with smaller snow cover changes around 2000 m a.s.l. In spring, however, no significant linear correlation is found ($r = 0.04, p > 0.05$; Fig. 8e), despite the presence of a well-defined elevation-dependent structure, with maximum surface temperature changes occurring between approximately 1500 and 2000 m a.s.l., coinciding with snow cover changes of about 50–70%. This pattern indicates that the relationship between snow cover and temperature is non-linear (Mackiewicz 2012), particularly in spring, and strongly modulated by elevation. The non-linearity likely arises from differences in the statistical distributions of the two variables and from threshold processes in snow–temperature interactions, which may also involve an important role of snowmelt (Castellanos et al. 2026). In particular, spring conditions are characterized by a transitional regime in which snow cover becomes highly sensitive to temperature variations, where the snow–albedo feedback can play a dominant role (Beaumet et al. 2021; Napoli et al. 2023a) and may contribute to shaping the elevation-dependent pattern of surface temperature changes.

5.6 Links between radiative balance and surface temperature

Changes in the shortwave radiation and net radiative budget are well correlated with surface temperature changes in MAM, with correlation coefficients of $r = 0.70$ ($p < 0.05$) and $r = 0.63$ ($p < 0.05$), respectively (see Fig. 8q, s). In DJF, no linear correlation higher than 0.5 is found between

surface temperature and either longwave or net radiative budget (Fig. 7r, s), while a moderate correlation is observed for the shortwave budget ($r = 0.55, p < 0.05$; Fig. 7q). The relatively weaker correlations in DJF are partly explained by the fact that the relationship is not strictly linear. When accounting for the nonlinearity of the signal, both the shortwave and net radiative balances exhibit clear elevation-dependent patterns consistent with surface temperature changes: larger increases in ts correspond to stronger positive shortwave changes. This pattern is more pronounced in MAM than in DJF. These results suggest that variations in the net radiative budget are primarily driven by changes in the shortwave component, while the longwave contribution plays a secondary role. This interpretation is consistent with previous studies showing that longwave radiation is expected to change in response to variations in temperature, atmospheric humidity, and cloud cover (e.g., Liu et al. 2025). Although longwave downwelling radiation represents a major contribution to changes in surface net radiation (Ohmura 2024), both downward and upward longwave components tend to increase simultaneously under warming conditions (see Fig. 5). Consequently, changes in net longwave radiation exhibit smaller variations compared to changes in net shortwave radiation (see Fig. 6), which shows larger spatial and temporal variability due to its strong dependence on cloud and surface properties (Wild et al. 2013). The pattern with the elevation is consistent with increasing shortwave-driven energy accumulation at higher elevations, which in turn leads to enhanced surface warming. This behavior could be linked to mechanisms associated with high-elevation environments, such as snow cover changes in the region (Matiu et al. 2021; Beaumet et al. 2021) by the reduction in surface albedo (Thackeray et al. 2019) across different elevation bands (Winter et al. 2017). In addition, changes in land surface properties could also explain the observed pattern, particularly through soil moisture control on near-surface temperature (Seneviratne et al. 2006, 2010), although the relative contribution of these processes cannot be directly assessed from the present analysis.

5.7 Links between heat fluxes and surface temperature

CMIP5 and EURO-CORDEX projections for Central Europe indicate substantial future changes in the surface energy budget, with a strong seasonal re-partitioning between latent and sensible heat fluxes driven by changes in soil moisture and precipitation regimes (Skalák et al. 2025). These changes are generally more pronounced during the spring season, consistent with enhanced evapotranspiration and the combined effects of temperature and precipitation variability. Over the European Alps in DJF, no significant correlation with surface temperature is found for either latent heat flux (hfls) or sensible heat flux (hfss) (see Fig. 7o, p). However, a not linear elevation-dependent signal emerges: higher elevations are associated with stronger increases in ts, a positive change in sensible heat flux, and a weak positive change in latent heat flux. In contrast, lowland areas, characterized by smaller changes in ts, exhibit predominantly negative sensible heat flux changes and strongly positive latent heat flux variations. In MAM (see Fig. 8o, p), stronger correlations with ts are observed for both fluxes ($r = 0.57, p < 0.05$ for hfls; $r = 0.54, p < 0.05$ for hfss), although no clear elevation-dependent pattern is detected. This pattern characterizes the surface heat fluxes and is primarily driven by soil moisture availability and snow cover conditions, while sublimation and snowmelt processes also play an important role (Castellanos et al. 2026). In DJF, at high elevations where snow is present, increases in surface temperature occur while snow cover limits the response of latent heat flux, leading to a stronger increase in sensible heat flux. In contrast, low-elevation areas exhibit weaker increases in ts and a tendency toward higher latent heat flux and reduced sensible heat flux, potentially associated with differences in soil moisture availability and precipitation regimes (Fig. 4). In MAM, the onset of snowmelt alters the surface conditions, leading to a different coupling between ts and surface heat fluxes.

6 Conclusions

Although local features arise from the complex topography, geographical configuration, and spatial heterogeneity of the mountain range, identifying large-scale patterns of change across the region is crucial for understanding how climate is evolving in the European Alps and how it affects its dense population as well as various socio-economic and environmental sectors.

Beyond using surface temperature as a valuable diagnostic variable to identify the dominant physical drivers of temperature changes, the findings of this study highlight the critical role of minimum temperatures (tasmin) in driving changes in the Diurnal Temperature Range (DTR) in the European Alpine Region, with a more pronounced reduction at higher elevations during winter (DJF) and spring (MAM) seasons. Specifically, tasmin changes exhibit a strong correlation with surface temperature (ts) changes in winter and spring, indicating that nocturnal variations are closely linked to surface processes, when the stable stratification of the Planetary Boundary Layer limits mixing. Moreover, larger increases in tasmin and ts are projected at higher elevations compared to low elevations.

The influence of tasmin is particularly pronounced at higher elevations, where variations in specific humidity (huss) and downward longwave radiation (rlds) show strong correlations with ts changes in DJF. This highlights how relatively small absolute changes at high elevations can substantially amplify the effect of longwave radiation on surface temperature under future conditions. In spring, these correlations slightly weaken but remain significant, suggesting a shift in the dominant controls on surface temperature. During this season, changes in snow cover fraction and soil properties at higher elevations may modulate the surface radiative balance, with a comparatively stronger role of shortwave radiation than in winter. In addition, both soil properties and snow cover emerge as key drivers of surface heat flux variability, which in turn influences surface temperature variability.

Overall, our findings indicate that while RCM outputs are generally consistent and informative, they should be interpreted as a first-order approximation (see Supplementary Material, Sections S1 and S2). This is particularly relevant in high-elevation environments, where careful consideration is required to ensure that model outputs adequately support adaptation strategies. A further limitation of this study is that the development of regional climate models is beyond our control, preventing a full assessment of whether all relevant processes are properly represented and how they interact. Moreover, the large model domain limits the ability to resolve specific mountain systems in detail.

To further refine these insights and better capture local-scale processes, sensitivity analyses based on high-resolution model ensembles such as CORDEX-FPS (Ban et al. 2021; Pichelli et al. 2021), together with complementary idealized experimental frameworks, are needed to disentangle the underlying mechanisms and their interactions. Moreover, diagnosing the full energy balance in the RCM outputs, including snowmelt and heat conduction within the snowpack and soil layers, would be necessary to better understand surface–atmosphere interactions. Finally, future analyses could examine changes in the other two seasons, summer (June–August) and autumn (September–November), as well as potential elevation-dependent shifts in the magnitude of change. Such approaches would help assess whether the patterns identified in this study persist at finer spatial and temporal scales and clarify the processes driving them, providing further insight into the mechanisms of climate change in mountain regions, ultimately enhancing our understanding of climate dynamics in complex terrain and supporting more robust adaptation strategies.

Supplementary Information The online version contains supplementary material available at https://doi.org/10.1007/s00382-026-08305-x.

Acknowledgements We acknowledge Prof. Claudia Pasquero for the insightful comments and discussion about mechanisms at play, and Prof. Nick Pepin for the discussions about different elevation patterns of weather variables during Anna Napoli's stay as a visiting scholar at the University of Portsmouth. Moreover, we acknowledge the World Climate Research Programme's Working Group on Regional Climate, and the Working Group on Coupled Modelling, former coordinating body of CORDEX and responsible panel for CMIP5. We also thank the climate modelling groups for producing and making available their model output. We acknowledge the Earth System Grid Federation infrastructure, an international effort led by the U.S. Department of Energy's Program for Climate Model Diagnosis and Intercomparison, the European Network for Earth System Modelling and other partners in the Global Organisation for Earth System Science Portals (GO-ESSP). We acknowledge the Italian Ministry of Education, Universities and Research (MUR) framework of the project DICAM-EXC (Departments of Excellence 2023-2027, grant L232/2016). Anna Napoli has been supported by "Fondazione CARITRO" (Cassa di Risparmio di Trento e Rovereto) within the project "Insight into the physical mechanisms underlying convection phenomena for a better understanding of its future evolution in the context of climate change in the Trentino region" which is acknowledged. Bruno Majone, Dino Zardi, and Alberto Bellin also acknowledge support from "iNEST (Interconnected Nord-Est Innovation Ecosystem)" project funded by the European Union under NextGenerationEU (PNRR, Mission 4.2, Investment 1.5, Project ID: ECS 00000043). Dino Zardi acknowledges support from the Italian Ministry for University and Research (MUR) under the project "DECIPHER–Disentangling mechanisms controlling atmospheric transport and mixing processes over mountain areas at different space- and timescales," funded by the scheme "Research Projects of Relevant National Interest–Call 2022 (PNRR2022)," CUPE53D23004450006, Code protocol 2022NEWP4J.

Author Contributions Anna Napoli, Michael Matiu, and Sven Kotlarski contributed to the study conception and design. Data collection was performed by Michael Matiu. Data analysis was performed by Anna Napoli. A first draft of the manuscript was written by Anna Napoli, and all authors contributed to subsequent modifications that led to the final submitted version. All the authors approved the final version of the paper.

Funding Open access funding provided by Università degli Studi di Trento within the CRUI-CARE Agreement. This research received financial support from the project "Sintesi degli studi sui cambiamenti climatici e i loro impatti ed elaborazione di scenari climatici di riferimento per il Trentino" funded by the Agency for Environmental Protection (Agenzia Provinciale per la Protezione dell'Ambiente, APPA) of the Autonomous Province of Trento, Italy.

Data Availability No new data were generated. Source of analysed data can be found in the methods description.

Code Availability All code used in the analysis will be publicly made available on https://github.com/tnclima/.

Declarations

Conflict of interest The authors declare no competing interests.

Ethics approval and consent to participate Not applicable

Consent for publication Not applicable

Open Access This article is licensed under a Creative Commons Attribution 4.0 International License, which permits use, sharing, adaptation, distribution and reproduction in any medium or format, as long as you give appropriate credit to the original author(s) and the source, provide a link to the Creative Commons licence, and indicate if changes were made. The images or other third party material in this article are included in the article's Creative Commons licence, unless indicated otherwise in a credit line to the material. If material is not included in the article's Creative Commons licence and your intended use is not permitted by statutory regulation or exceeds the permitted use, you will need to obtain permission directly from the copyright holder. To view a copy of this licence, visit http://creativecommons.org/licenses/by/4.0/.

References

Auer I, Böhm R, Jurkovic A et al (2007) HISTALP–historical instrumental climatological surface time series of the Greater Alpine Region. Int J Climatol 27(1):17–46. https://doi.org/10.1002/joc.1377

Ban N, Lavín Gullón Á, Milovac J, et al (2021) The first multi-model ensemble of regional climate simulations at kilometer-scale resolution, part i: evaluation of precipitation https://doi.org/10.1007/s00382-021-05708-w

Barati AA, Zhoolideh M, Azadi H et al (2023) Interactions of land-use cover and climate change at global level: How to mitigate the environmental risks and warming effects. Ecol Ind 146:109829. https://doi.org/10.1016/j.ecolind.2022.109829

Bartolini E, Claps P, D'odorico P (2009) Interannual variability of winter precipitation in the european alps: relations with the north atlantic oscillation. Hydrol Earth Syst Sci 13(1):17–25. https://doi.org/10.5194/hess-13-17-2009

Barton BT, Schmitz OJ (2018) Opposite effects of daytime and nighttime warming on top-down control of plant diversity. https://doi.org/10.1002/ecy.2062

Beaumet J, Ménégoz M, Morin S et al (2021) Twentieth century temperature and snow cover changes in the french alps. Reg Environ Change 21(4):114. https://doi.org/10.1007/s10113-021-01830-x

Bertò A, Buzzi A, Zardi D et al (2004) Back-tracking water vapour contributing to a precipitation event over trentino: a case study. Meteorol Z 13(3):189–200. https://doi.org/10.1127/0941-2948/2004/0013-0189

Bigi A, Ghermandi G, Harrison RM (2012) Analysis of the air pollution climate at a background site in the po valley. J Environ Monit 14(2):552–563. https://doi.org/10.1016/j.atmosenv.2010.02.028

Bilgili M, Tokmakci M (2025) Climate change and trends in europe and globally over the period 1970–2023. Physics and Chemistry of the Earth Parts A/B/C 139:103928. https://doi.org/10.1016/j.pce.2025.103928

Blanchet J, Blanc A, Creutin JD (2021) Explaining recent trends in extreme precipitation in the southwestern alps by changes in atmospheric influences. Weather and Climate Extremes 33:100356. https://doi.org/10.1016/j.wace.2021.100356

Bongiovanni G, Matiu M, Crespi A et al (2024) Eear-clim: A high density observational dataset of daily precipitation and air temperature for the extended european alpine region. Earth System Science Data Discussions 2024:1–32. https://doi.org/10.5194/essd-17-1367-2025

Brönnimann S, Rajczak J, Fischer EM et al (2018) Changing seasonality of moderate and extreme precipitation events in the alps. Nat Hazard 18(7):2047–2056. https://doi.org/10.5194/nhess-18-2047-2018

Castellanos I, Ménégoz M, Blanchet J et al (2026) Projected elevation-dependent warming in the alps: contrasting free-atmosphere and surface trends with surface energy balance drivers. Earth System Dynamics 17(3):581–605. https://doi.org/10.5194/esd-17-581-2026

Ceppi P, Scherrer SC, Fischer AM et al (2012) Revisiting swiss temperature trends 1959–2008. Int J Climatol 32(2):203–213. https://doi.org/10.1002/joc.2260

CH2018 (2018) CH2018 - Climate Scenarios for Switzerland. Technical Report, National Centre for Climate Services, Zurich, ISBN: 978-3-9525031-4-0

Cheng J, Xu Z, Zhu R et al (2014) Impact of diurnal temperature range on human health: a systematic review. Int J Biometeorol 58:2011–2024 https://doi.org/10.1007/s00484-014-0797-5

Coppola E, Nogherotto R, Ciarlo' JM, et al (2021) Assessment of the European Climate Projections as Simulated by the Large EURO-CORDEX Regional and Global Climate Model Ensemble. Journal of Geophysical Research: Atmospheres 126(4):e2019JD032356. https://doi.org/10.1029/2019JD032356

Crespi A, Matiu M, Bertoldi G et al (2021) A high-resolution gridded dataset of daily temperature and precipitation records (1980–2018) for Trentino-South Tyrol (north-eastern Italian Alps). Earth System Science Data 13(6):2801–281. https://doi.org/10.5194/essd-13-2801-2021, https://essd.copernicus.org/articles/13/2801/2021/, publisher: Copernicus GmbH

Edwards AC, Scalenghe R, Freppaz M (2007) Changes in the seasonal snow cover of alpine regions and its effect on soil processes: a review. Quatern Int 162:172–181. https://doi.org/10.1016/j.quaint.2006.10.027

Fayad A, Gascoin S, Faour G et al (2017) Snow hydrology in mediterranean mountain regions: A review. J Hydrol 551:374–396. https://doi.org/10.1016/j.jhydrol.2017.05.063

Ferguglia O, Palazzi E, Arnone E (2024) Elevation dependent change in era5 precipitation and its extremes. Clim Dyn 62(8):8137–8153. https://doi.org/10.1007/s00382-024-07328-6

Frei P, Kotlarski S, Liniger MA et al (2018) Future snowfall in the Alps: projections based on the EURO-CORDEX regional climate models. Cryosphere 12(1):1–2. https://doi.org/10.5194/tc-12-1-2018, https://tc.copernicus.org/articles/12/1/2018/, publisher: Copernicus GmbH

Gallou A, Jump AS, Lynn JS et al (2023) Diurnal temperature range as a key predictor of plants' elevation ranges globally. Nat Commun 14(1):7890. https://doi.org/10.1038/s41467-023-43477-8

Giovannini L, Davolio S, Zaramella M et al (2021) Multi-model convection-resolving simulations of the october 2018 vaia storm over northeastern italy. Atmos Res 253:105455. https://doi.org/10.1016/j.atmosres.2021.105455

Gobiet A, Kotlarski S, Beniston M et al (2014) 21st century climate change in the European Alps–A review. Sci Total Environ 493:1138–115. https://doi.org/10.1016/j.scitotenv.2013.07.050, http://www.sciencedirect.com/science/article/pii/S0048969713008188

Guariso G, Volta M (2017) Air Quality Integrated Assessment: A European Perspective. Springer Nature https://link.springer.com/book/10.1007/978-3-319-33349-6

Guo H, Wang X, Guo Z et al (2026) Latitude/elevation-dependent response of snow phenology to climate change in the northern hemisphere from 1972 to 2022. J Hydrology p 135331. https://doi.org/10.1016/j.hydrol.2026.135331

Hiebl J, Frei C (2018) Daily precipitation grids for Austria since 1961–development and evaluation of a spatial dataset for hydroclimatic monitoring and modelling. Theoret Appl Climatol 132(1):327–34. https://doi.org/10.1007/s00704-017-2093-x

IPCC A, Chap W (2021) Changing state of the climate system. Clim Change 2021–The Phys Sci Basis 287–422. https://doi.org/10.1017/9781009157896.004

Isotta FA, Frei C, Weilguni V et al (2014) The climate of daily precipitation in the Alps: development and analysis of a high-resolution

grid dataset from pan-Alpine rain-gauge data. Int J Climatol 34(5):1657–167. https://doi.org/10.1002/joc.3794
Jacob D, Petersen J, Eggert B et al (2014) EURO-CORDEX: new high-resolution climate change projections for European impact research. Reg Environ Change 14(2):563–57. https://doi.org/10.1007/s10113-013-0499-2
Jacob D, Teichmann C, Sobolowski S et al (2020) Regional climate downscaling over europe: perspectives from the euro-cordex community. Reg Environ Change 20:1–20. https://doi.org/10.1007/s10113-020-01606-9
Kotlarski S, Gobiet A, Morin S et al (2022) 21st Century alpine climate change. Climate Dynami. https://doi.org/10.1007/s00382-022-06303-3
Kuhn M, Olefs M (2020) Elevation-dependent climate change in the european alps. Oxford research encyclopedia of climate science. https://doi.org/10.1093/acrefore/9780190228620.013.762
Liu L, Huang Y, Gyakum JR (2025) Clouds reduce downwelling longwave radiation over land in a warming climate. Nature 637(8047):868–874. https://doi.org/10.1038/s41586-024-08323-x
Mackiewicz MC (2012) A new approach to quantifying soil temperature responses to changing air temperature and snow cover. Polar Sci 6(3–4):226–236. https://doi.org/10.1016/j.polar.2012.06.003
Mall RK, Chaturvedi M, Singh N et al (2021) Evidence of asymmetric change in diurnal temperature range in recent decades over different agro-climatic zones of india. Int J Climatol 41(4):2597–2610. https://doi.org/10.1002/joc.6978
Manara V, Brunetti M, Celozzi A et al (2016) Detection of dimming/brightening in italy from homogenized all-sky and clear-sky surface solar radiation records and underlying causes (1959–2013). Atmos Chem Phys 16(17):11145–11161. https://doi.org/10.5194/acp-16-11145-2016
Marty C (2013) Climate change and snow cover in the european alps. In: The impacts of skiing and related winter recreational activities on mountain environments. Bentham Science Publishers, p 30–44 https://doi.org/10.2174/978160805488611301005
Marty C, Schlögl S, Bavay M et al (2017) How much can we save? Impact of different emission scenarios on future snow cover in the Alps. Cryosphere 11(1):517–52 https://doi.org/10.5194/tc-11-517-2017, http://www.the-cryosphere.net/11/517/2017/
Matiu M, Crespi A, Bertoldi G et al (2021) Observed snow depth trends in the european alps: 1971 to 2019. Cryosphere 15(3):1343–1382. https://doi.org/10.5194/tc-15-1343-2021
Ménégoz M, Valla E, Jourdain NC et al (2020) Contrasting seasonal changes in total and intense precipitation in the european alps from 1903 to 2010. Hydrol Earth Syst Sci 24(11):5355–5377. https://doi.org/10.5194/hess-24-5355-2020
Napoli A, Crespi A, Ragone F et al (2019) Variability of orographic enhancement of precipitation in the alpine region. Sci Rep 9(1):13352. https://doi.org/10.1038/s41598-019-49974-5
Napoli A, Desbiolles F, Parodi A et al (2022) Aerosol indirect effects in complex-orography areas: a numerical study over the great alpine region. Atmos Chem Phys 22(6):3901–3909. https://doi.org/10.5194/acp-22-3901-2022
Napoli A, Parodi A, von Hardenberg J et al (2023a) Altitudinal dependence of projected changes in occurrenceof extreme events in the great alpine region. Int J Climatol 12:5813–5829. https://doi.org/10.1002/joc.8222
Napoli A, Pepin N, Palazzi E, et al (2023b) A workshop on advances in our understanding of elevation dependent climate change. Bulletin of the American Meteorological Society 104(4):E928–E934. https://doi.org/10.1175/BAMS-D-23-0043.1
Napoli A, Matiu M, Laiti L et al (2026) Building the scientific basis for the adaptation strategy of an alpine region: The 'state of the climate in trentino'report. Climate Services 41:100629. https://doi.org/10.1016/j.cliser.2025.100629
Nigrelli G, Chiarle M (2023) 1991–2020 climate normal in the european alps: focus on high-elevation environments. J Mt Sci 20(8):2149–2163. https://doi.org/10.1007/s11629-023-7951-7
Ohmura A (2024) Decadal variation of longwave downwelling and net radiation as observed at the surface with implication for climate sensitivity: Based on pyrgeometer and pyranometer measurements. Journal of the European Meteorological Society 1:100003. https://doi.org/10.1016/j.jemets.2024.100003
Palazzi E, Filippi L, von Hardenberg J (2017) Insights into elevation-dependent warming in the tibetan plateau-himalayas from cmip5 model simulations. Clim Dyn 48(11):3991–4008. https://doi.org/10.1007/s00382-016-3316-z
Palazzi E, Mortarini L, Terzago S et al (2019) Elevation-dependent warming in global climate model simulations at high spatial resolution. Clim Dyn 52(5):2685–270. https://doi.org/10.1007/s00382-018-4287-z
Pepin N, Bradley RS, Diaz HF et al (2015) Elevation-dependent warming in mountain regions of the world. Nat Clim Chang 5(5):424–43. https://doi.org/10.1038/nclimate2563
Pepin N, Maeda EE, Williams R (2016) Use of remotely sensed land surface temperature as a proxy for air temperatures at high elevations: Findings from a 5000 m elevational transect across kilimanjaro. Journal of Geophysical Research Atmospheres 121(17):9998–10 https://doi.org/10.1002/2016JD025497
Pepin N, Apple M, Knowles J, et al (2025) Elevation-dependent climate change in mountain environments. Nature Reviews Earth & Environment pp 1–17 https://doi.org/10.1038/s43017-025-00740-4
Pepin NC, Arnone E, Gobiet A, et al (2022) Climate Changes and Their Elevational Patterns in the Mountains of the World. Reviews of Geophysics 60(1):e2020RG000730. https://doi.org/10.1029/2020RG000730
Pichelli E, Coppola E, Sobolowski S et al (2021) The first multi-model ensemble of regional climate simulations at kilometer-scale resolution part 2: historical and future simulations of precipitation. Clim Dyn 56(11):3581–3602. https://doi.org/10.1007/s00382-021-05657-4
Pogliotti P, Cremonese E, Cella UM (2023) Warming permafrost in the western alps: a further evidence of elevation dependent warming? J Alp Research| Revue de géographie Alp 111–112. https://doi.org/10.4000/rga.11784
Ramtvedt EN, Bollandsås OM, Næsset E et al (2021) Relationships between single-tree mountain birch summertime albedo and vegetation properties. Agric For Meteorol 307:10847. https://doi.org/10.1016/j.agrformet.2021.108470 , https://www.sciencedirect.com/science/article/pii/S0168192321001532
Rangwala I (2013) Amplified water vapour feedback at high altitudes during winter. Int J Climatol 33(4):897–90. https://doi.org/10.1002/joc.3477
Rogora M, Arisci S, Mosello R (2004) Recent trends of temperature and precipitation in alpine and subalpine areas in north western italy. Geogr Fis Dinam Quat 27:151–158. https://www.gfdq.glaciologia.it/index.php/GFDQ/article/view/389
Rottler E, Vormoor K, Francke T, et al (2021) Elevation-dependent compensation effects in snowmelt in the Rhine River Basin upstream gauge Basel. Hydrology Research (nh2021092). https://doi.org/10.2166/nh.2021.092
Rysman JF, Lemaître Y, Moreau E (2016) Spatial and temporal variability of rainfall in the alps-mediterranean euroregion. J Appl Meteorol Climatol 55(3):655–671. https://doi.org/10.1175/JAMC-D-15-0095.1
Scherrer SC, Isotta FA, Kotlarski S (2026) Elevation-dependent warming in switzerland: Observed signals and dataset limitations. Journal of the European Meteorological Society 4:100026. https://doi.org/10.1016/j.jemets.2025.100026

Schicker I, Radanovics S, Seibert P (2010) Origin and transport of mediterranean moisture and air. Atmos Chem Phys 10(11):5089–5105. https://doi.org/10.5194/acp-10-5089-2010

Schilliger L, Tetzlaff A, Bourgeois Q, et al (2024) An investigation on causes of the detected surface solar radiation brightening in europe using satellite data. Journal of Geophysical Research: Atmospheres 129(15):e2024JD041101. https://doi.org/10.1029/2024jD041101

Schmidli J, Schmutz C, Frei C et al (2002) Mesoscale precipitation variability in the region of the european alps during the 20th century. International Journal of Climatology A Journal of the Royal Meteorological Society 22(9):1049–1074. https://doi.org/10.1002/joc.769

Seneviratne SI, Lüthi D, Litschi M et al (2006) Land-atmosphere coupling and climate change in europe. Nature 443(7108):205–209 https://doi.org/10.1038/nature05095

Seneviratne SI, Corti T, Davin EL et al (2010) Investigating soil moisture-climate interactions in a changing climate: A review. Earth Sci Rev 99(3):125–16. 2010.02.004. https://doi.org/10.1016/j.earscirev.2010.02.004 , https://www.sciencedirect.com/science/article/pii/S0012825210000139

Shati F, Prakash S, Norouzi H et al (2018) Assessment of differences between near-surface air and soil temperatures for reliable detection of high-latitude freeze and thaw states. Cold Reg Sci Technol 145:86–92. https://doi.org/10.1016/j.coldregions.2017.10.007

Skalák P, Meitner J, Fischer M et al (2025) The projected changes in the surface energy budget of the cmip5 and euro-cordex models: are we heading toward wetter growing seasons in central europe? J Hydrometeorol 26(4):481–499. https://doi.org/10.1175/JHM-D-24-0017.1

Škrk N, Serrano-Notivoli R, Čufar K et al (2021) Sloclim: a high-resolution daily gridded precipitation and temperature dataset for slovenia. Earth System Science Data 13(7):3577–3592. https://doi.org/10.5194/essd-13-3577-2021

Sodemann H, Zubler E (2010) Seasonal and inter-annual variability of the moisture sources for alpine precipitation during 1995–2002. International Journal of Climatology A Journal of the Royal Meteorological Society 30(7):947–961. https://doi.org/10.1002/joc.1932

Thackeray CW, Derksen C, Fletcher CG et al (2019) Snow and Climate: Feedbacks, Drivers, and Indices of Change. Current Climate Change Reports 5(4):322–33. https://doi.org/10.1007/s40641-019-00143-w

Toledo O, Palazzi E, Toro C, IM (2021) Comparison of elevation-dependent warming and its drivers in the tropical and subtropical andes. Clim Dyn 1–18. https://doi.org/10.1007/s00382-021-06081-4

Tudoroiu M, Eccel E, Gioli B et al (2016) Negative elevation-dependent warming trend in the Eastern Alps. Environ Res Lett 11(4):04402. https://doi.org/10.1088/1748-9326/11/4/044021 , publisher: IOP Publishing

Valt M, Cianfarra P (2010) Recent snow cover variability in the Italian Alps. Cold Reg Sci Technol 64(2):146–15. https://doi.org/10.1016/j.coldregions.2010.08.008, http://www.sciencedirect.com/science/article/pii/S0165232X10001540

Vautard R, Kadygrov N, Iles C, et al (2021) Evaluation of the Large EURO-CORDEX Regional Climate Model Ensemble. Journal of Geophysical Research: Atmospheres 126(17):e2019JD032344. https://doi.org/10.1029/2019JD032344

Wang YR, Samset BH, Stordal F et al (2023) Past and future trends of diurnal temperature range and their correlation with vegetation assessed by modis and cmip6. Sci Total Environ 904:166727. https://doi.org/10.1016/j.scitotenv.2023.166727

Weber RO, Talkner P, Auer I (1997) 20th-century changes of temperature in the mountain regions of central europe. Climatic Change at High Elevation Sites pp 95–112. https://doi.org/10.1023/A:1005378702066

Wild M, Folini D, Schär C et al (2013) The global energy balance from a surface perspective. Clim Dyn 40(11):3107–3134. https://doi.org/10.1007/s00382-012-1569-8

Williamson SN, Zdanowicz C, Anslow FS (2020) Evidence for elevation-dependent warming in the st. elias mountains, yukon, canada. J Clim 33(8):3253–3269. https://doi.org/10.1175/JCLI-D-19-0405.1

Winter KJPM, Kotlarski S, Scherrer SC et al (2017) The Alpine snow-albedo feedback in regional climate models. Clim Dyn 48(3):1109–112. https://doi.org/10.1007/s00382-016-3130-7

Zampieri M, Scoccimarro E, Gualdi S (2013) Atlantic influence on spring snowfall over the alps in the past 150 years. Environ Res Lett 8(3):034026. https://doi.org/10.1088/1748-9326/8/3/034026

Zandonai A, Fontana V, Klotz J et al (2024) Six years of high-resolution climatic data collected along an elevation gradient in the italian alps. Scientific Data 11(1):751. https://doi.org/10.1038/s41597-024-03580-x

Zhang M, Gao Y, Ting M et al (2024) Land-use induced changes in extreme temperature predominantly influenced by downward longwave radiation. Communications Earth & Environment 5(1):758. https://doi.org/10.1038/s43247-024-01936-0

Zhao P, He Z, Ma D et al (2024) Temperature trends and its elevation-dependent warming over the qilian mountains. J Mt Sci 21(2):500–510. https://doi.org/10.1007/s11629-023-8449-z

Publisher's Note Springer Nature remains neutral with regard to jurisdictional claims in published maps and institutional affiliations.